ANALYSIS OF CFC WING-SPAR WITH LOCAL CUTOUTS

K. Panbarasu; V.R. Ranganath
CSIR National Aerospace Laboratories
HAL Airport Road, Post Box No. 1779
Bangalore-560 017, India
Email : panbuu@nal.res.in; panbuu@yahoo.com

T.C. Subba Reddy; K. Vijayaraju
Aeronautical Development Agency
Vimanapura Post, Post Box No. 1718
Bangalore-560 017, India

R. Shanmugham
MVJ College of Engineering
Bangalore-560 067, India

Abstract

In multi-cell aircraft wing construction, cutouts and vent-holes are commonly provided in the wing spars and ribs to facilitate fuel transfer across cells. While the web of the spar is expected to transfer shear loads under an overall bending load, presence of such discontinuities are of great concern. In particular, wing spars made of fiber reinforced composites, such discontinuities may result in fiber terminations and are well known locations of stress concentration. Present work attempts to analyze a carbon fiber composite (CFC) wing spar, with cutouts and vent-holes, under fixed beam conditions with the load applied through the shear centre of the spar to induce a pure bending stress at the cutout, through FE analysis and with a limited number of experiments. The study includes C-spars with and without skin-strips made of carbon fiber composites, and the cutout loaded in, both, tension and compression. The strain data measured extensively during the tests was employed to identify stress concentrations, critical failure locations and failure modes. The study establishes the need for modeling the whole loading assembly to achieve results close to experimental results.

***Keywords**: Composites, FEM analysis, CFC wing spar, cutouts*

Introduction

Laminated composites are increasingly used in primary aircraft structures, such as the wing spars and ribs, as they offer higher stiffness and strength to weight ratio compared to their metallic counterparts. These composite panels often require cutouts for functional access, eg., inspection, looming of electric and fuel lines, as well as for reducing the structural weight. Cutouts lead to stress concentration and reduced buckling load capability. Therefore, the effects of cutouts on laminated composite panels have been investigated by many researchers over the last 40 years.

The effects of a cutout on the buckling behavior of rectangular plates made of polymer matrix composites (PMC) have been studied on the behavior of rectangular symmetric cross-ply laminates [1]. Key findings include the effects of cutout size, shape, plate aspect ratio and boundary conditions. An analytical investigation to study the stress analysis of plates with different central cutouts, the effect of geometry (circular, square or special cutouts), material properties (isotropic and orthotropic), fiber angles, and cutout curvature is also reported [2]. The presented method indicates that FEM can be used to determine accurately the stresses and stress concentration in composite plates with special shape cutouts. Guo [3] has investigated the effectiveness of different types of reinforcements around a circular cutout in terms of reduction in stress concentration and improvement in critical buckling load of a composite shear panel. The study has shown that the most significant reduction in stress concentration and the best improvement in buckling stability can be obtained by a pair of rings (doublers) attached to each side of the cutout. Eiblmeier [4] and Loughlan [5] studied the

buckling response of a laminate panel with a circular cutout reinforced by doublers under different loading and boundary conditions. This investigation showed that buckling stability increases most efficiently with rings up to 15mm wide. The magnitude of stress reduction was found to be strongly related to the stiffness of the reinforcement rings. The diamond-shaped cutout and the fiber tows reinforcement show clear advantages over the widely adapted circular cutout and laminated ring reinforcement [6].

This paper reports a recent investigation into the design of reinforcement skin with a combination of two different laminates of a typical composite C-spar used in supersonic fighter aircraft wings. The objective is to find the effect of varying stiffness on stress concentration around the cutout regions, the stiffness, in turn, is varied by altering the stacking sequence of the laminates. Another variable that was studied is the effect of reinforcement skins. The combinations of spar stiffness along with the skin stiffness are compared. The failure load and the failure locations are predicted through FEA using the Tsai-Wu criteria.

Materials and Methods

Material

Typical carbon-epoxy pre-pregs (T300-914C) of 0.15mm ply thickness were employed for fabrication of the C-spar test specimen and FEA models were also carried out for the same. Tables-1 and 2 show the mechanical properties of the lamina and the layup details respectively.

The C-Section Beams

The C-spar is of 675mm long, 3mm thick, with a fillet radius of 5mm, flange width of 30mm and height as 150mm having seven vent holes of 10mm diameter each spaced at a gap of 100mm. The fuel transfer cutout (designed to give optimum fuel transfer even at low fuel level) is of triangular shape and provides lower stress concentration factor around the cutout region [2]. The dimensional details of the spar are shown in Fig.1.

Test Parameters

As discussed in the introduction, the failure location and the failure loads can be altered by changing the layup sequence of the plies or by adding a reinforcement skin to the flange. Accordingly, four cases of spar construction are considered in this study. Since the load has to be applied through the shear centre of the spar, and the C section of the spar is an open section, the shear centre of the section lies away from the spar web. Shear centre and the moment of inertia of the individual configurations were calculated and are shown in Table-3.

Loading Conditions

The C-spar considered for the analysis will be in the span-wise direction of the wing. The ribs run between these spars and the aerodynamic loads acting on the wing are transferred to the spars through these ribs. Essentially, the spar is a fixed beam between the ribs, taking transverse loads. The bending stresses are reacted by the flanges and the shear stresses are reacted by the web of the spar. The cutout, situated in the web, being the weakest link is to be examined closely. For this, a fixed beam with load line on

Table-1 : Mechanical Properties of Lamina*

E_1, GPa	E_2, GPa	G_{12}, GPa	ν_{12}	X_t, MPa	X_c, MPa	Y_t, MPa	Y_c, MPa	S, MPa	ρ, kg/m^3
130	10	5	0.35	1200	1000	40	246	65	1800

* E_i : ply modulus in the i-direction; G_{ij} : ply shear modulus in the i-j plane ; ν_{ij} : ply Poisson's ratio in the i-j plane ; ρ : density; X_t, X_c : tensile/compressive strength in fiber direction; Y_t, Y_c : tensile/compressive strength in transverse direction; S : shear strength

Table-2 : Laminate Lay-up Details

Lay-up Id	Lay-up	E_1, GPa	E_2, GPa	G_{12}, GPa	ν_{12}	No. of Layers
17	$[\pm45/\pm45/\pm45/\pm45/\pm45]_s$	17.62	17.62	33.57	0.762	20
33	$[\pm45/\pm45/\pm45/\pm45/0/90]_s$	33.25	33.25	27.85	0.552	20
Skin	$[45/0/-45/90]_{4s}$	50.8	50.8	19.3	0.316	32

Table-3 : Details of Test Cases

Case	Id	Description	Laminate Stiffness, GPa	Moment of Inertia, mm^4	Shear Centre, mm
1	WoS-17	Spar without skin	17.62	1719036	7.66
2	WoS-33	Spar without skin	33.25	1719036	7.66
3	WS-17	Spar with skin	17.62	3559987	10.57
4	WS-33	Spar with skin	33.25	3559987	10.57

the shear center, with suitable boundary conditions, as shown in Fig.2(a), was considered to simulate maximum shear in the web. This analysis would also lead to a conservative estimation of critical stresses.

During bending the top flange of the C-spar experiences compressive loading and the bottom flange experiences tension loading, hence two load cases, tension and compression are considered for the study. Load case definition, namely tension or compression, is defined with respect to the stresses prevailing near the fuel transfer cut-out in the spar as shown in Fig.2. Under tensile loading the vent holes will be near the flange which is undergoing compressive stress, where as the fuel transfer cutout will be nearer to the other flange which is undergoing tensile stress. The reverse is true when the compressive load is applied on the spar. For ease of description, the vent holes are numbered H_1 to H_7, starting from left to right and the triangular cutout is termed as TC.

Modeling Approach

The finite element analysis of the C-spar is carried out using MSC-PATRAN and MSC-NASTRAN. For defining the properties of all the layers of the composite laminate, as discussed in Section - Material, PCOMP card of the NASTRAN library is employed. Two dimensional quadrilateral linear shell elements of type CQUAD4 and the IsoMesh facility are used for meshing the C-spar. The QUAD4 elements are capable of modeling composite properties. The regions around the vent holes and fuel transfer cutout are fine meshed [7] with a size of about 1/10 of the elements employed elsewhere, and provided a good convergence. Material properties, boundary and loading conditions were implemented in the model using the appropriate tools offered by PATRAN. Typical FE model of a spar without skin and with skin has 14357 and 15929 shell elements respectively.

Calibration of FEM Model

Initially the spar was modeled and load is applied through shear centre using the appropriate FEM technique. It was found that the deflection was not matching well within a decent range when compared with experimentally obtained data. Afterwards when the fixture, which was used for the testing, was also modeled through FEM, the deflection and other results matched well with experimental data. Therefore it is suggested here that to reduce assumptions in the modeling, it is beneficial to model the whole loading assembly, such as fixtures, couplings, etc., and that FEM outputs be matched with limited experimental data at the beginning of a detailed analysis. A comparison of the FEA results and the experimental results in terms of strains at some critical locations are shown in Fig.3 along with the details of strain gage (SG) locations and the nomenclature.

Results and Discussion

Stress Concentration Around the Cutouts

A load of 20kN (tension) was applied and the X-component stresses (σ_x) for all the four cases of the spar (average from a total of 20 layers) are shown in Fig. 4. The maximum stresses appear at vent holes and cutout regions. The stress distribution around these regions is subjected to a detailed analysis as shown in Table-4 and Fig.5.

A comparison of stresses around H_1, H_3, H_4, H_7 and TC for the cases of with skin and without skin, shows that nearer to the load/reaction points (Fig.2a) a clear difference is observed, with the former showing lower stress. At the maximum stress location (H_4) the order of reduction is about 40%, as can be expected, when skin reinforcement is provided. When the stiffness is varied (layup stacking sequence) the difference is not significant. Also, it is observed that high tensile stresses prevail at the triangular cutout (TC) and high compressive stresses at the vent holes H_3 and H_4. The trend gets reversed when compressive load

Table-4 : Stress Magnitude Around the Cutouts (σ_x, MPa)

Stress	Case	Description	H_1	H_2	H_3	H_4	H_5	H_6	H_7	TC
Tensile (T)	1	WoS-17	66	90	81	75	44	84	52	144
	2	WoS-33	62	68	85	82	49	61	52	138
	3	WS-17	33	94	79	53	58	75	26	111
	4	WS-33	36	73	76	60	52	57	32	112
Compressive (C)	1	WoS-17	47	84	195	196	106	51	36	96
	2	WoS-33	37	76	216	226	122	42	31	87
	3	WS-17	26	104	130	115	92	71	22	105
	4	WS-33	25	90	152	148	103	57	22	92

is applied, that is the stress magnitude remains the same while the sign changes.

However, when the stresses are compared at the maximum locations, it is interesting to note that in both cases of with skin (case 4) and without skin (case 2), increasing the spar stiffness increases the stress around the hot spots [8]. A comparison of the values as in Table-4 and Fig.5, for all the four cases illustrates this point. In composites the layup sequence of the laminate plays a vital role in altering the local stresses and strains [9].

Failures in composite structures can be classified as by either strength or stiffness dominated. Strength limited failures occur when unit stress exceeds the load carrying capability of the laminate. Stiffness failures result when displacements exceed the strain limits (elongation to failure) of the laminate. It has been reported [9] that in a composite laminate the fibers oriented in 0° can sustain maximum load and fibers oriented in 90° sustain the least load for failure.

In ±45° layups, such as load cases 1 and 3 the deflection becomes predominant criteria than the load to cause the failure. It follows that in both cases 2 and 4, the first ply fails earlier than the others, since it has 90° layers. The differences between the stresses on first ply and plies further down are significant [10]. In the case of 1 and 3 configurations, for the same applied load of 20kN, the first ply and further plies experience the same level of stress. The designer would prefer ±45° type of layup for the composite laminates where significant deflections are expected, such as in wing constructions.

Failure Indices (FI) and Margin of Safety (MoS)

Having analyzed the stress concentration around the cutouts, the main failure criteria for all the cases can be considered. For this purpose Tsai-Wu failure criterion has been chosen because it is a phenomenological failure theory which is widely used for anisotropic composite materials which have strengths differing in tension and compression [9]. This is supplemented by a maximum criterion for through-thickness shear load causing matrix failure, and margins of safety are given by:

$$\text{MoS} = \text{SR}-1, \text{ where SR (strength ratio)} = 1/\text{FI} \quad (1)$$

Table-5 provides a summary of failure indices (FI), margin of safety (MoS) and their locations. To be on the conservative side, the results are shown for failure of only the first ply.

It is observed from Table-4 and Table-5 that for composite spars the location of failure index and the X-component stresses (σ_x) for the laminates are in good agreement. From this, it is clear that the location of X-component stresses (σ_x), where the magnitude of stress is significantly high can be the deciding criteria to determine the exact failure location.

In composite laminates, location of failure also depends on the orientation of the layers and a fixed location of failure may be determined like in isotropic materials. As can be seen from the analysis so far, the sizing of the vent holes and cutout radii would influence not only the stress distribution but also the stress concentration factor (SCF) due to the radii. Thus, a combination of layup, positioning, SCF and the nature of load (compression/tension) would influence the failure location.

Table-5 : Results of FI and MoS

Load, 20kN	Case	Id	FI	MoS, %	Location
Tension	1	WoS-17	1.46	-31.5	H_4
	2	WoS-33	1.07	-6.5	H_4
	3	WS-17	0.633	58	H_3
	4	WS-33	0.641	56	TC
Compression	1	WoS-17	2.13	-53	H_4
	2	WoS-33	1.75	-42.9	H_4
	3	WS-17	0.76	31.6	H_4
	4	WS-33	0.967	3.4	H_4

Conclusions

- FEA model was successfully generated that is demonstrated through a comparison of predicted values and experimental data.
- The stress/strain alteration due to changes in the spar design (cutouts, vent holes, skin reinforcement, etc.) can be visualized confidently through this analysis.
- Stress concentration studies in the spar cutouts reveal that the cutouts that are nearer to the flange are critical.
- The hot spots that are identified from stress analysis are in good agreement with the prediction of failure locations for first ply failure.
- A combination of skin design and the layup orientation of laminate have a synergistic effect on failure of a composite structure. Increase in the stiffness improves sustainability, when there is no skin reinforcement. However, when skin reinforcement is provided, the trend gets altered based on the skin design.

Acknowledgement

The assistance rendered by the contract staff and technical staff of FSIG has been crucial in fabrication, strain gauging and data logging that is sincerely acknowledged. Discussion with various scientists of the CSIR-NAL has helped in clearing some of the issues that cropped up during the investigation. Sincere thanks are due for the ADA Management, Head (STTD, CSIR-NAL) and the Director, CSIR-NAL for their encouragement to carry out the work and to permit the submission of the paper.

References

1. Ghannadpour, S.A.M., Najafi, A. and Mohammadi, B., "On the Buckling Behavior of Cross Ply Laminated Composite Plates Due to Circular/elliptical Cutouts", Jl. Comp. Strs., No.75, 2006, pp.3-6.

2. Rezaeepazhand, J. and Jafari, M., "Stress Analysis of Perforated Composite Plates", Jl. Comp. Strs., No.71, 2005, pp.463-468.

3. Guo, S., "Stress Concentration and Buckling Behavior of Shear Loaded Composite Panels with Reinforced Cutouts", Jl. Comp. Strs., No.80, 2007, pp.1-9.

4. Eiblmeier, J. and Loughlan, J., "The Buckling Response of Carbon Fibre Composite Panels with Reinforced Cutouts", Jl. Comp. Strs., No.32, 1995, pp.97-113.

5. Eiblmeier, J. and Loughlan, J., "The Influence of Reinforcement Ring Width on the Buckling Response of Carbon Fibre Composite Panels with Circular Cutouts", Jl. Comp. Strs., No.38, 1997, pp.609-622.

6. Guo, S., Morishima, R., Zhang, X. and Mills, A., "Cutout Shape and Reinforcement Design for Composite C-section Beams Under Shear Load", Jl. Comp. Strs., No.88, 2009, pp.179-187.

7. Henshaw, J.M., Sorem, J.R. and Glaessgen, E.H., "Finite Element Analysis of Ply-by-Ply and Equivalent Stress Concentrations in composite plates with

multiple Holes Under Tensile and Shear Loading, Jl. Comp. Strs., No.36, 1996, pp.45-48.

8. Mahase H. and Whitworth, H.A., "Failure of Orthotropic Plates Containing a Circular Opening", Jl. Comp. Strs., No.46, 1999, pp.53-57.

9. Robert M. Jones., "Mechanics of Composite Materials", Second Edition, 1999, Taylor and Francis Inc.

10. Panbarasu, K., "Analysis of Perforated CFC Wing Spar", M. Tech Thesis, MVJ Engineering College, Bangalore, 2010.

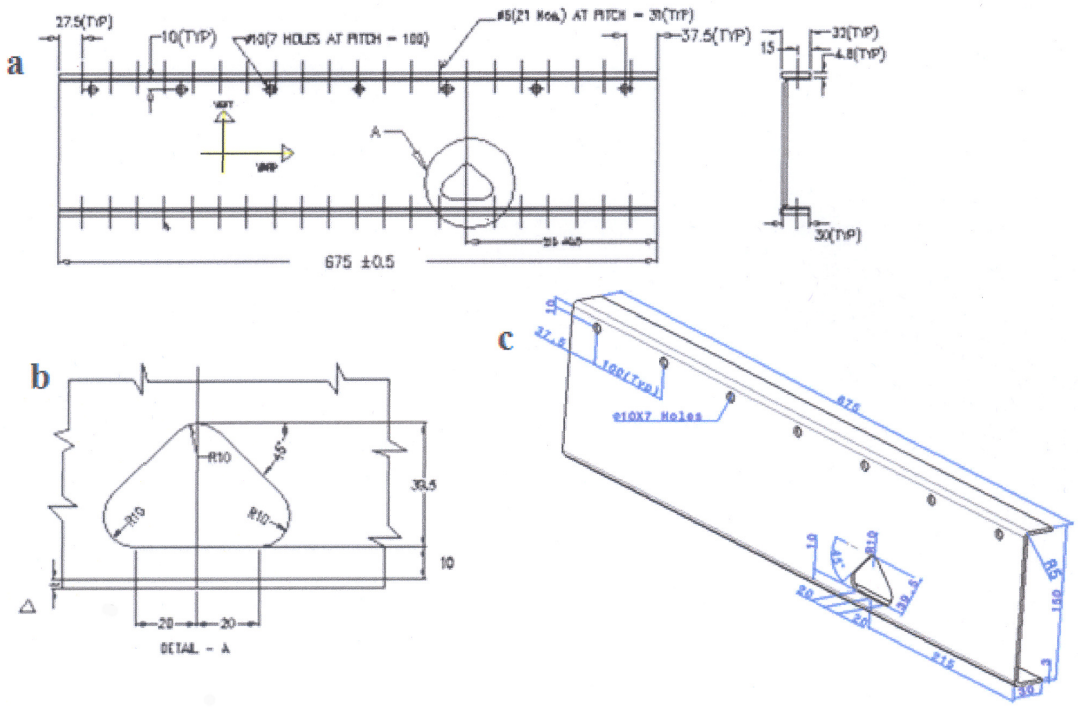

Fig.1 (a) Dimensional Details of Spar with Skin, (b) Detail at A and (c) Spar without skin

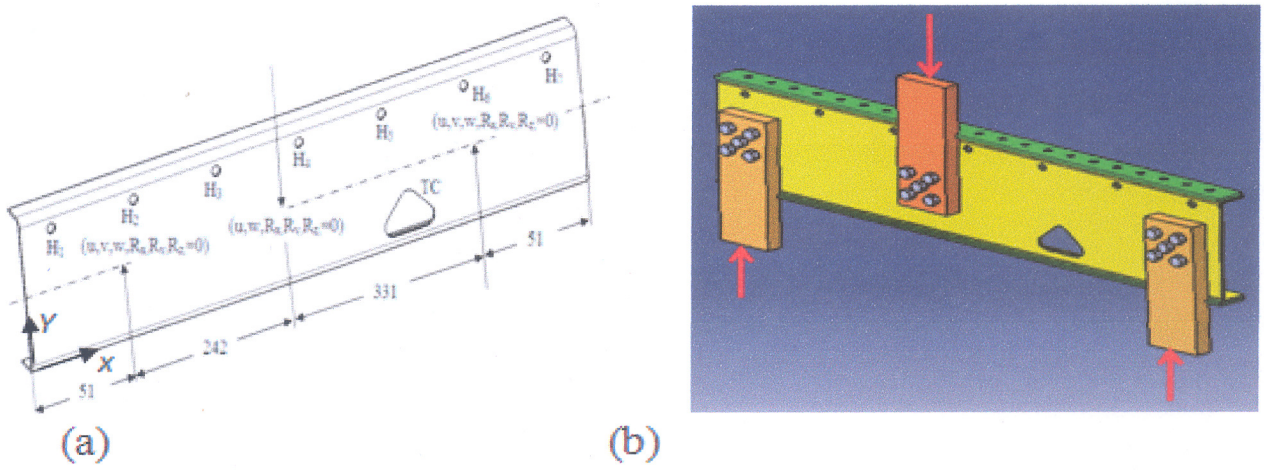

Fig.2 (a) Details of Load and Boundary Conditions, (b) Load Bracket Assembly Employed for Testing and Modeling

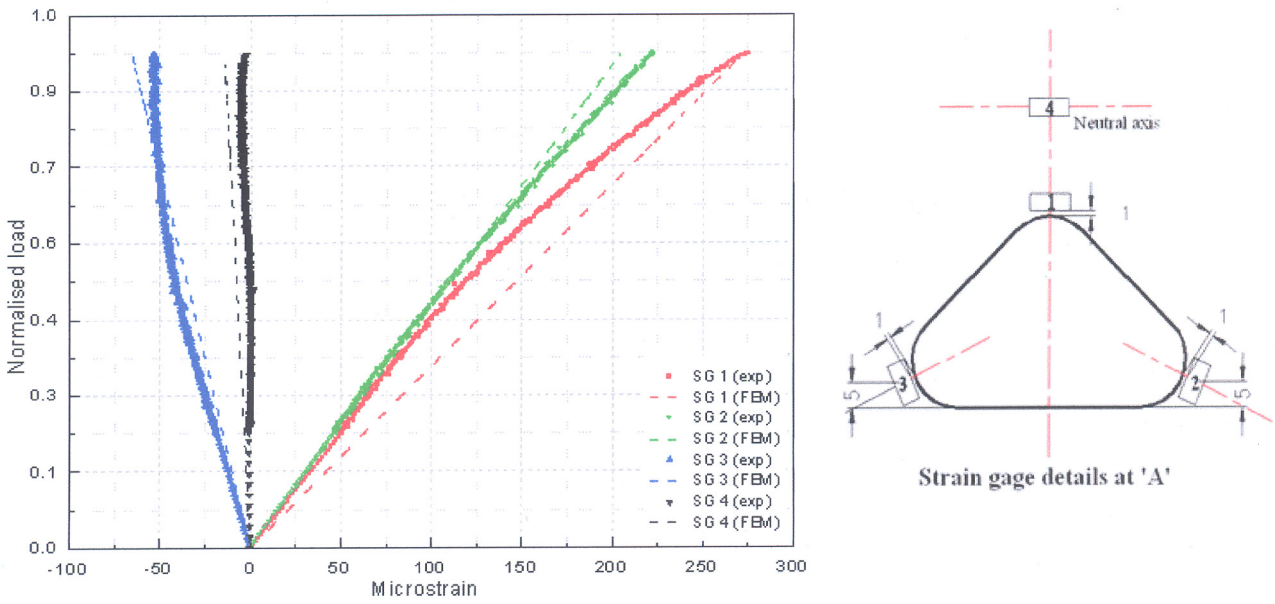

Fig.3 Comparison of Experimental and FEM Load vs Strain Data at Critical Locations (Case 4)

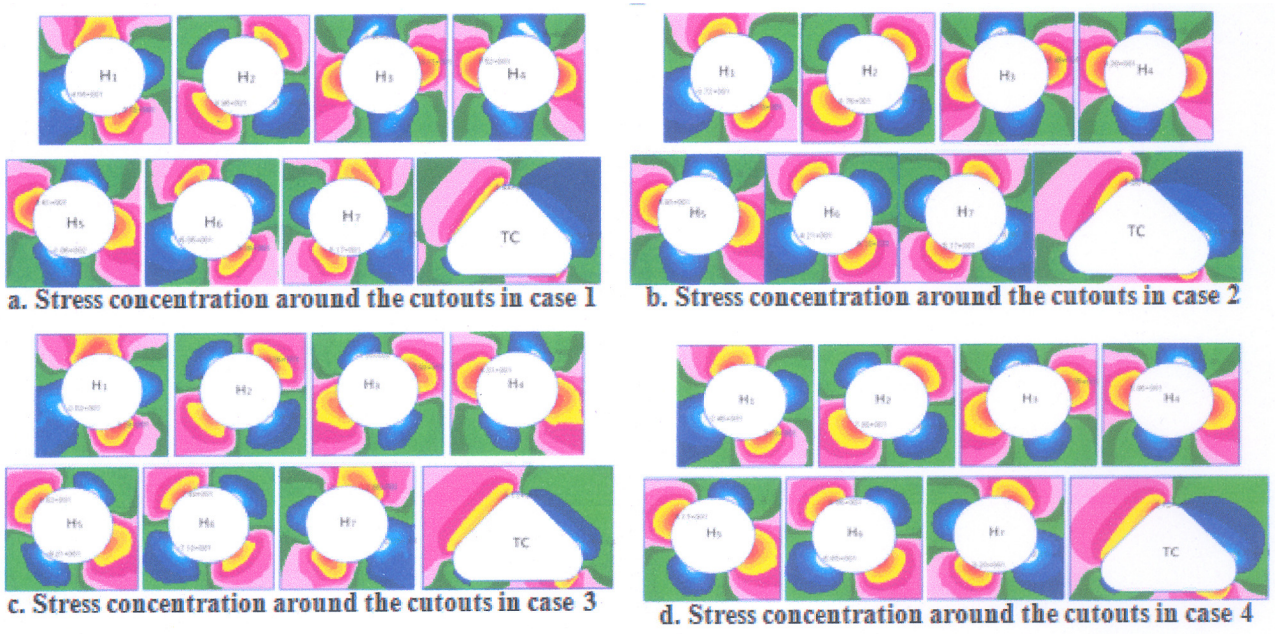

Fig.4 Stress Distribution (X-Component, σ_x) Around the Cutout Regions of all the Cases Under Consideration

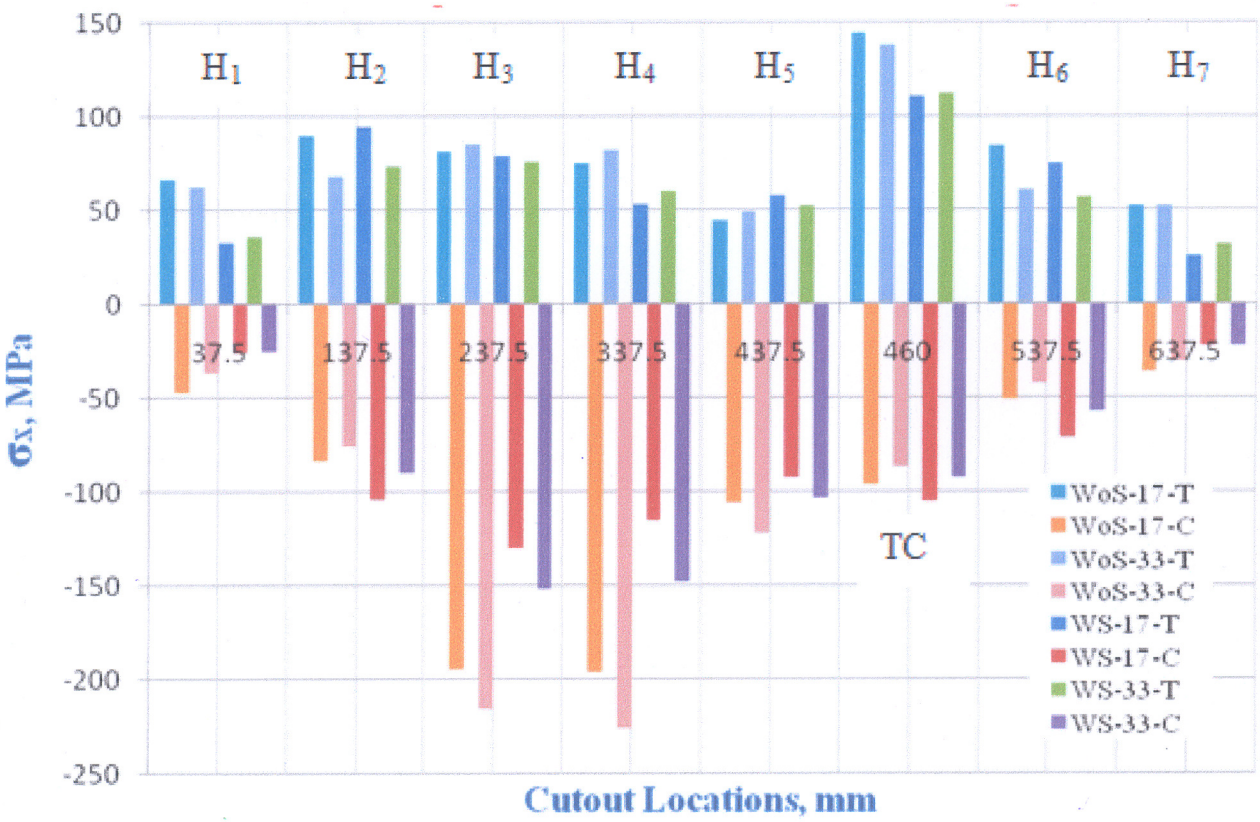

Fig.5 Stress Concentration Around the Cutouts Over the Length of Spar